



Numerical model of a thermoacoustic engine

Omar Hireche^a, Catherine Weisman^{a,b,*}, Diana Baltean-Carlès^{a,b}, Patrick Le Quéré^a,
Maurice-Xavier François^{a,b}, Luc Bauwens^c

^a Laboratoire d'informatique pour la mécanique et les sciences de l'ingénieur, UPR CNRS 3251, BP 133, 91403 Orsay cedex, France

^b Université Pierre et Marie Curie-Paris 6, 4, place Jussieu, 75252 Paris cedex 05, France

^c University of Calgary, Department of Mechanical and Manufacturing Engineering, 2500 University Drive NW, Calgary, AB T2N 1N4, Canada

ARTICLE INFO

Article history:

Received 20 March 2009

Accepted after revision 4 December 2009

Available online 8 January 2010

Presented by Sébastien Candel

Keywords:

Computational fluid dynamics

Thermoacoustics

Low Mach

Numerical simulation

Wave amplification

Mots-clés :

Mécanique des fluides numérique

Thermoacoustique

Faible Mach

Simulation numérique

Amplification

ABSTRACT

An asymptotically consistent small Mach number model of a standing wave thermoacoustic engine has been developed. A simple thermoacoustic engine consists of a resonating tube within which is inserted an acoustically compact assembly, composed of a stack of conducting plates, placed between two heat exchangers. The model couples one-dimensional linear acoustics in the resonator with a low Mach number viscous and conducting flow in the stack/heat exchangers section. The latter is solved through a two-dimensional numerical simulation. Results show that the model successfully captures the dynamics of the starting process, at a much lower cost than a fully compressible simulation of the entire engine.

© 2009 Académie des sciences. Published by Elsevier Masson SAS. All rights reserved.

R É S U M É

Cette étude présente un modèle numérique pour la simulation du démarrage d'un moteur thermoacoustique à onde stationnaire. Ce modèle couple une solution analytique des équations de l'acoustique linéaire dans le résonateur, avec une approximation faible Mach des équations de Navier–Stokes dans le domaine comprenant le stack et les échangeurs de chaleur. La résolution numérique de ces dernières est effectuée par un code volume-finis bidimensionnel. Les résultats obtenus montrent que le modèle reproduit bien la dynamique du processus d'amplification de l'onde, pour un coût bien inférieur à celui d'une simulation d'un écoulement compressible dans tout le moteur.

© 2009 Académie des sciences. Published by Elsevier Masson SAS. All rights reserved.

1. Introduction

A typical thermoacoustic engine consists of a resonant tube closed at one end and equipped with a load at the other end, within which a heat exchanger section is placed. The heat exchanger section is made up of a heater and a cooler, separated by a stack made of flat plates of conducting material, along which surface heat pumping occurs. When the temperature gradient in the stack plates exceeds some critical value the gas inside the tube becomes unstable and starts to oscillate. Thus thermal energy is transformed into acoustic energy, under a thermoacoustic mechanism, and the device operates as a heat engine.

Thermoacoustic instability was first observed by Taconis [1]: when a small tube was inserted in a cryostat, large oscillations would develop, leading to rapid evaporation of liquid helium. The classical model due to Rott [2] couples longitudinal

* Corresponding author at: Laboratoire d'informatique pour la mécanique et les sciences de l'ingénieur, UPR CNRS 3251, BP 133, 91403 Orsay cedex, France.

E-mail address: catherine.weisman@limsi.fr (C. Weisman).

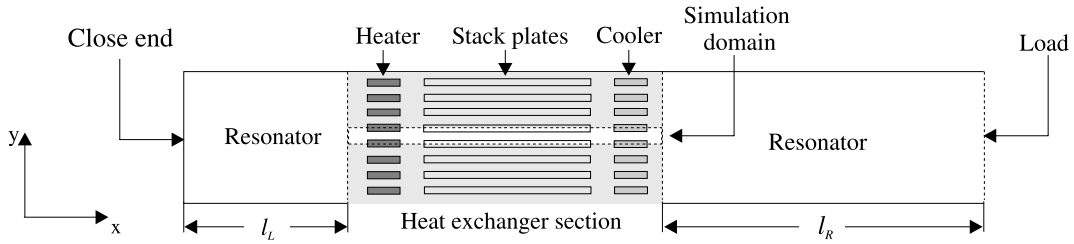


Fig. 1. Geometry.

acoustics with a boundary layer solution. More recent analysis by Swift [3], mostly based upon the Rott formulation focuses upon stationary operation. Most analytical works [4–8] still ignore many two-dimensional effects in the heat exchangers.

For efficient operation, the length of the stack, hence the length over which the temperature gradient is present, should be comparable to the sweep due to the oscillating fluid motion. Thus the set of heat exchangers, including stack, should be acoustically compact, i.e. shorter than the acoustic wavelength by a factor of the order of the flow Mach number. Then, the same velocities which appear in an acoustic context in the resonator (the remainder of the long tube) belong in a small Mach number flow model in the heat exchanger section. However, large temperature gradients occur, due to the large temperature difference that is imposed between the hot and cold heat exchangers. These flows might also support potentially large spatially uniform pressure fluctuations. Since in the current device, forcing is acoustic, these fluctuations will remain small, though. Flows like these occur in regenerators [9] and also in combustion in closed vessels [10–12].

Alternating engines require a resonance; here it is provided by interaction between fluid inertia and compressibility. As long as the resulting velocities remain smaller than the speed of sound (beyond which efficiency drops rapidly), the flow in the resonator will be acoustic. This flow, in which velocities and period are similar in two regions, respectively the heat exchanger section and the oscillator, with lengths in a ratio of the order of the Mach number, lends itself naturally to a multiple scales analysis.

An exact closed form solution to the resonator acoustics is thus coupled with a direct numerical simulation for the transient, viscous and conducting flow in the stack and heat exchangers. A description of the numerical solution follows, and finally, results are presented.

2. Physical model

2.1. Initial–boundary value problem

The geometry of the device consists of a duct with rectangular cross-section within which a stack of plates, sandwiched between a cold and a hot heat exchanger, is inserted, as shown in Fig. 1.

Transient operation of this device is represented by an initial–boundary value problem, characterized by conservation of mass, momentum and energy, including viscosity and conduction, for a known compressible fluid. Temperature is specified on the heat exchanger walls. In the stack walls, energy is conserved, and temperature and heat flux are continuous along the stack walls. No-slip boundary conditions apply on the stack and heat exchanger walls. One end is closed, on the left in Fig. 1. At the other end, the load is characterized by a known relationship between the acoustic pressure on the end wall, and the velocity of the moving tube end.

The problem also requires an initial condition. Clearly, for balanced temperatures if initially the fluid is at rest, it will remain at rest. Thus the problem is in effect a stability problem. Initial conditions including not only the thermodynamic state but also some (possibly zero) initial velocities must be provided. The initial stack temperature and fluid temperature need to be specified.

This problem can be solved numerically without further simplification [13–15]. However, this entails very large computations, in which the time steps will be limited to very small values by an acoustic CFL condition. However, as long as the Mach number remains small, flow in the resonators will differ very little from linear acoustics. In contrast, in the heat exchanger section, there is a need for a simulation that deals with transient and spatially resolved velocities and temperatures. An appropriate simplified model that concentrates the numerical work on the heat exchanger section can be formally derived from multiple scale analysis.

All variables are scaled uniformly throughout the device except for the spatial coordinates which are scaled in the heat exchanger section by the stack length L_S , and in the resonator by the resonator length L_R , with $L_S \ll L_R$. Time is scaled by an acoustic reference, defined as $t_{ref} = L_R/a_{ref}$, where a_{ref} is the speed of sound at the reference temperature T_{ref} (equal to the cold temperature). The reference velocity is defined as $U_{ref} = L_S/t_{ref}$. This results in a reference Mach number $M = U_{ref}/a_{ref} = L_S/L_R$, which is typically on the order of 10^{-3} . Therefore a small Mach number model will yield results that will be quite accurate. Dimensionless variables are introduced by scaling pressure by the mean pressure P_{ref} , temperature by T_{ref} and all thermophysical variables (density, viscosity, ...) by their values defined at reference pressure and temperature. Variables without superscript correspond to leading order values.

2.2. Resonator model

Since in the resonator, oscillating boundary layers are thin compared with width, the flow is approximately one-dimensional. In the scaling introduced above, it is governed by the usual inviscid, non-conducting, isentropic acoustics formulation. A d'Alembert solution is readily formulated using Riemann variables $\mathcal{L} = \gamma u - \sqrt{T} p^{(1)}$, and $\mathcal{R} = \gamma u + \sqrt{T} p^{(1)}$. \mathcal{L} is constant on characteristics moving left at the speed of sound, and \mathcal{R} on characteristics moving right. Here the temperature T takes different values on the two sides of the heat exchanger section (denoted as T_L for the left side and T_R for the right side), u is velocity, γ is the specific heats ratio and $p^{(1)}$ is the acoustic pressure, i.e. a perturbation of order M to the mean pressure.

At the closed end, $u = 0$. Thus, given that $\mathcal{L} + \mathcal{R} = 2\gamma u$, \mathcal{R}_L at the left end of the heat exchanger section at time t is related to \mathcal{L}_L at the same location at t minus the round-trip travel time to the left end of the resonator (l_L being the distance to the left end):

$$\mathcal{R}_L(t) = -\mathcal{L}_L(t - 2l_L/\sqrt{T_L}) \quad (1)$$

At the other end, the exact moving wall boundary condition is readily replaced by an equivalent condition at a fixed location, corresponding to a load described as an impedance f such that $p^{(1)} = fu$. In the same way as on the left end, this leads to a reflection:

$$\mathcal{L}_R(t) = Z\mathcal{R}_R(t - 2l_R/\sqrt{T_R}), \quad Z = \frac{\gamma - f\sqrt{T_R}}{\gamma + f\sqrt{T_R}} \quad (2)$$

An open end corresponds to $f = 0$ while at a closed end, f is infinite, both cases resulting in a zero load. Finite non-zero values of f correspond to a finite non-zero load, which has a damping effect. The current acoustic model itself does not include losses. As a result it provides no damping effect.

2.3. Heat exchanger section

Scaling the conservation laws as above except for length which is now scaled by L_S results in a viscous, conducting low Mach number model for an ideal gas, that supports spatially homogeneous pressure fluctuations up to leading order, in which temperatures and densities may vary at leading order and in which dynamically induced pressure gradients only occur at order M^2 . In effect, the approximation obtained is the same as in [9–11], and in the context of thermoacoustic heat pumping, in [16,17]. However, given that the acoustic model in the resonator only produces pressure fluctuations at order M , in the current problem, pressure remains constant at leading order. The dynamic viscosity μ , thermal conductivity k and heat capacity c_p are considered to be temperature independent. Gravity is neglected. The dimensionless equations become:

$$\frac{\partial \rho}{\partial t} + \nabla \cdot \rho \mathbf{u} = 0 \quad (3)$$

$$\frac{\partial (\rho \mathbf{u})}{\partial t} + \nabla \cdot (\rho \mathbf{u} \otimes \mathbf{u}) = -\nabla p^{(2)} + \frac{1}{Re} \nabla \cdot \tau \quad (4)$$

$$\rho \left[\frac{\partial T}{\partial t} + (\mathbf{u} \cdot \nabla) T \right] = \frac{1}{Pe} \nabla^2 T \quad (5)$$

$$p = 1 = \rho T \quad (6)$$

where $p^{(2)}$ is the perturbation of order M^2 to the mean pressure, $\tau = [\nabla \mathbf{u} + (\nabla \mathbf{u})^t - \frac{2}{3}(\nabla \cdot \mathbf{u})\mathbf{I}]$, the reference Reynolds number is $Re = \rho_{ref} U_{ref} L_S / \mu_{ref}$ and the reference Péclet number is $Pe = \rho_{ref} c_{pref} U_{ref} L_S / k_{ref}$. In the solid plates the dimensionless heat conduction equation is:

$$\frac{\partial T}{\partial t} = \frac{1}{Pe_s} \nabla^2 T \quad (7)$$

where the solid Péclet number is defined as $Pe_s = Pe \alpha_{ref} / \alpha_s$, α_{ref} and α_s being thermal diffusivities respectively at the reference state in the fluid and in the solid.

Although this is a low Mach number flow, because leading order density variations occur, energy conservation cannot be decoupled from conservation of mass and momentum. Viscous dissipation does not appear in the leading order energy equation because its contribution only occurs at order M^2 . Conductive losses are present at leading order and one readily checks that they provide for an entropy source at leading order, hence damping.

2.4. Matching relations

In the outer (acoustic) scaling, the heat exchanger section has a negligible length; in the inner scaling, the resonators have a length that $\rightarrow \infty$. Matching the two solutions, first, since at order lower than M^2 , the flow in the heat exchanger

section only supports spatially uniform pressure fluctuations, the inner section is transparent to acoustic pressure, which occurs at order M . However, integrating the energy equation over the entire fluid domain in the heat exchanger section, taking into account continuity and the equations of state equations, using the divergence theorem, and considering the normal boundary conditions $\mathbf{u} \cdot \mathbf{n} = 0$ on all boundaries except at the entrance and exit of the heat exchanger section domain, one finds that

$$H(u_L - u_R) + \frac{1}{Pe} \int \nabla T \cdot \mathbf{n} ds = 0 \quad (8)$$

Here, u_L corresponds to a location $x \rightarrow -\infty$ in the scaling associated with the heat exchanger section, but to the heat exchanger end of the left side of the resonator. Likewise, u_R corresponds to a location $x \rightarrow \infty$ in the scaling associated with the heat exchanger section, but to the heat exchanger end of the right side of the resonator. H is the spacing between two successive plates. Thus, while being transparent to acoustic (order M) pressure, the stack and heat exchanger section acts as a source of velocity in the acoustics, and therefore couples the inner and outer problems.

Taking into account that $p^{(1)}$ is spatially uniform in the heat exchanger section, Eq. (8), together with the acoustic solution above—Eq. (1) and Eq. (2)—provide velocity boundary conditions for $x \rightarrow -\infty$ and $x \rightarrow +\infty$ in the heat exchanger section, hence completing the low Mach number inner problem.

Finally, the flow is taken to be identical in all stack passages, allowing for simulation of only one passage (see Fig. 1).

3. Numerical solution

The numerical solution uses a finite volume solver initially developed for direct simulation of non-Boussinesq convection [18]. Treatment of diffusive terms is implicit while convection is explicit. The algorithm is second-order accurate in both space and time. A staggered mesh is used, with velocities defined on cell faces and state variables at cell centers. Continuity is ensured based upon a version of the projection method adapted for variable density, using a fractional step. The Helmholtz equations obtained for temperature and velocity components are solved using an ADI method. The equation for the dynamic pressure correction is solved by means of a multigrid method [19].

The presence of stack and heat exchanger walls is dealt with by introducing a phase variable that differentiates between fluid and solid, and ensures continuity of temperature and heat flux vector at the solid/fluid interfaces.

The simulation domain extends around the heat exchanger section, so that its length is twice the stack length. The matching equations are then written on the left and right domain boundaries, where the flow is forced to be one-dimensional.

At each time step, the resonator acoustics yield, on both sides of the stack and heat exchanger section, a relationship between velocity and acoustic pressure. Eq. (8) provides a third relationship, thus completing the necessary velocity boundary conditions.

4. Results

A device 7.87 m long with a 150 mm stack made of stainless steel plates 0.2 mm thick, separated by 0.77 mm, filled with helium at 1 MPa and 293 K on the cold side, is simulated. Heat exchangers are also made up of a stack of stainless steel plates, 7.5 mm long, that are aligned with the stack plates, with the same width, and the distance between heat exchanger and stack is equal to the stack passage width. The center of the heat exchanger section is located at 826 mm from the left end. This corresponds to a dimensionless description in which $L_R = 52.47L_S$, hence a reference Mach number of 0.019. These dimensions correspond to an actual device [20]. The large aspect ratio of the computational domain makes simulations difficult. Simulations have been performed on 1024×32 , 2048×32 and 2048×64 meshes.

Here, the focus is upon engine startup. To that effect, two different initial conditions have been used to represent engine start, respectively random noise, and a small amplitude monochromatic acoustic wave. However, the system being thermoacoustically unstable, oscillations can very easily be triggered, even for instance by numerical errors. Similar observations are made in experiments [4].

The natural resonance frequency of the resonator filled with ambient fluid and with no load is about 64 Hz. The corresponding period is 15.6 ms. The thermal conduction characteristic time, which needs to be resolved, is at least 10^6 times larger, making simulations rather challenging. Here time steps of $1/600$ of the period were used to simulate the initial amplification process. A time and space resolution study has been performed, showing the coarse grid to be adequate. The CPU time is about 1 μ s per time step and per mesh point on a NEC SX8. On a coarse grid, the average CPU time per run is 2 hours for the simulation of the phase of initial amplification.

The results presented were obtained for temperatures in a ratio 1.3, with infinite value of f (equivalent to a closed end on the right side also). In Figs. 2 to 4, a sinusoidal wave with frequency equal to the cold resonator fundamental natural frequency was used as initial condition. Fig. 2 shows the acoustic pressure time history, while Fig. 3 shows the shape of the signals and the phase differences between velocities and pressure over a narrow time window at the end of the run. Here time has been scaled by the period of the fundamental acoustic resonance in a cold tube with no load.

The two velocities are not very different, but they are clearly not identical, which is consistent with the signals still undergoing amplification. The signal is clearly non-sinusoidal; thus it contains multiple frequencies. This is in agreement

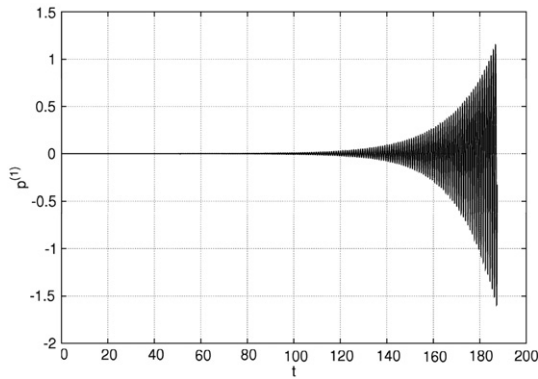


Fig. 2. Acoustic pressure term $p^{(1)}$ vs t .

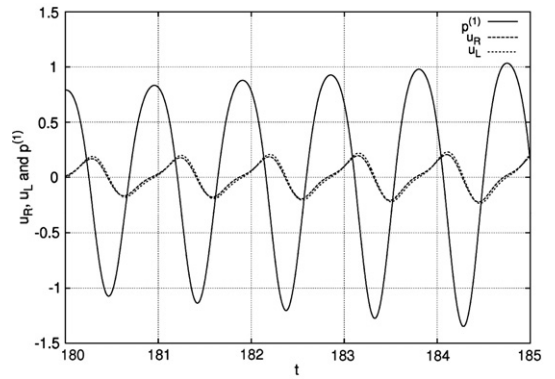


Fig. 3. $p^{(1)}$ and velocities u_L, u_R vs t .

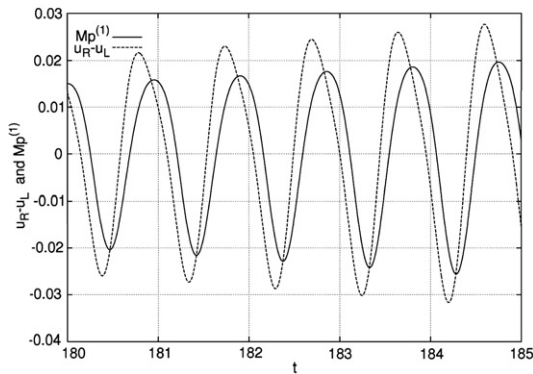


Fig. 4. Velocity difference across heat exchangers, and acoustic pressure $Mp^{(1)}$ vs t .

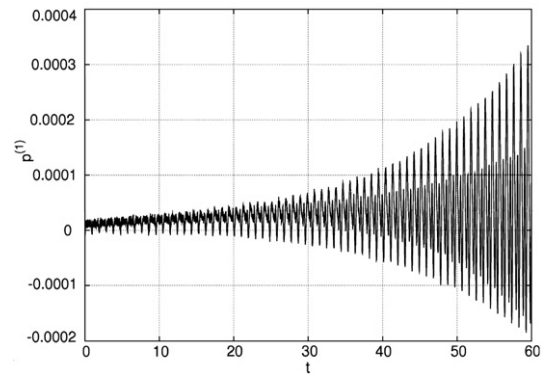


Fig. 5. $p^{(1)}$ vs t , random noise Incs.

with Rott’s linear theory [3]. The fundamental mode should correspond to the fundamental natural mode of the resonant tube taking into account that there is a temperature jump at the location of the heat exchangers, determined by the Lees/Rott dispersion relation [2,21]. However, given that the hot side of the resonator is relatively short, and that the temperature ratio is relatively low, these actual resonant frequencies will not differ significantly from those in a cold tube, and indeed the lowest frequency of oscillations is just over 1. It is the most energetic, due to the choice of initial excitation. The signal was also filtered to isolate the dominant modes and measure their associated growth rate, showing that the first harmonic, growing exponentially with growth rate $\sigma_2 = 4.43 \text{ s}^{-1}$, is slightly more unstable than the fundamental mode, with growth rate $\sigma_1 = 3.85 \text{ s}^{-1}$. Similar observations have been reported for some geometrical configurations in theoretical studies and in experiments [4,20].

The period is slightly different from the fundamental period of the acoustic oscillations not only because of the temperature jump, but also because of the presence of the heat exchanger section. The difference between the left and the right velocity amplitudes seen to some extent in Fig. 3, but much clearer in Fig. 4 also shows the heat exchangers performing as a heat engine. In the absence of amplification, the phase shift between pressure and left velocity is 90 degrees, since the wave on the left is a standing wave, with zero energy flux. Likewise, in the absence of amplification, the component in phase with pressure of the velocity difference shown in Fig. 4 provides a measure of the energy flux transmitted on the right side, toward the load.

Results in Fig. 4 correspond to the end of the computation. At that point in the amplification process, the drive ratio (acoustic pressure amplitude versus mean pressure) is 3.5% and dimensionless velocities are of order 0.25. Because velocities have grown considerably, in order to maintain the CFL close to unity, the simulation cannot be pursued without reducing the time step. This is the stability limit of the global algorithm owing to the implicit treatment of viscous part and explicit treatment of non-linear terms. Results shown are long enough to observe the amplification process, but the time window is too short for significant damping to be noticeable.

The results are virtually unchanged if random noise is used as initial condition (Fig. 5). Here, however, because there was no large initial deposition of energy into the fundamental mode, the first harmonic, which grows faster than the fundamental mode, is more energetic from early on in the simulation.

The current model only includes conductive losses but no viscous dissipation either in the heat exchanger section or in the resonators. Indeed, while in the heat exchanger section, diffusive terms appear in momentum, they do not appear at leading order in the energy or entropy balance, in contrast with conductive losses. When no load is applied (i.e. if both

resonator ends are closed), it appears that these are too small to significantly affect the onset of instability, at least within the time window that was simulated. The load positioned at the right resonator end absorbs energy; thus it acts as a resistive load, i.e. a dissipative element. Depending upon the value of this load, several situations are expected to occur: either the load will induce strong damping and the wave will eventually die out, or the system will stabilize at a fixed amplitude.

5. Conclusion

The current approach is a good example whereby the multiple scale technique can be used successfully, allowing the computational effort to be concentrated where it truly matters. The code that has been developed includes the key features of the device. Yet by virtue of not needing a numerical solution in the resonator, and by reducing the numerical model of the flow in the stack and heat exchangers to a low Mach number flow, the model that was implemented is orders of magnitude faster than numerical models dealing with the entire device using a compressible formulation. The results show that indeed the model is adequate and that it will allow for exploring the instability mechanism as well as engine efficiency, and the effect of crucial design parameters.

Acknowledgements

Support of the Natural Sciences and Engineering Research Council of Canada is gratefully acknowledged (LB). Computations were performed on the NEC-SX8 of the IDRIS-CNRS computing center, under project No. i2009020599.

References

- [1] K.W. Taconis, J.J.M. Beenakker, A.O.C. Nier, L.T. Aldrich, Measurements concerning the vapour-liquid equilibrium of solutions of He³ in He⁴ below 2.19 K, *Physica* 15 (8–9) (1949) 733–739.
- [2] N. Rott, Damped and thermally driven acoustic oscillations in wide and narrow tubes, *Z. Angew. Math. Phys.* 20 (1969) 230–243.
- [3] G.W. Swift, Thermoacoustic engines, *J. Acoust. Soc. Am.* 84 (1988) 1145–1180.
- [4] A.A. Atchley, H.E. Bass, T.J. Hofler, H.T. Lin, Study of a thermoacoustic prime mover below onset of self-oscillation, *J. Acoust. Soc. Am.* 91 (1992) 734–743.
- [5] S. Karpov, A. Prosperetti, Nonlinear saturation of the thermoacoustic instability, *J. Acoust. Soc. Am.* 107 (2000) 3130–3147.
- [6] V. Gusev, H. Baillet, P. Lotton, M. Bruneau, Asymptotic theory of nonlinear acoustic waves in a thermoacoustic prime-mover, *Acta Acustica* 86 (1999) 25–38.
- [7] M.F. Hamilton, Y.A. Ilinski, E. Zabolotskaya, Nonlinear two-dimensional model for thermoacoustic engines, *J. Acoust. Soc. Am.* 111 (2002) 2076–2086.
- [8] G. Penelet, V. Gusev, P. Lotton, M. Bruneau, Experimental and theoretical study of processes leading to steady-state sound in annular thermoacoustic engines, *Phys. Rev. E* 72 (2005) 016625–016625-13.
- [9] L. Bauwens, Oscillating flow of a heat-conducting fluid in a narrow tube, *J. Fluid Mech.* 324 (1996) 135–161.
- [10] S. Paolucci, On the filtering of sound from the Navier–Stokes equations, Sandia National Laboratories Report SAND82-8257, 1982.
- [11] A. Majda, J.A. Sethian, The derivation and numerical solution of the equations for zero Mach number combustion, *Combust. Sci. Tech.* 42 (1984) 185–205.
- [12] L. Bauwens, C.R.L. Bauwens, I. Wierzb, Oscillating flames: multiple-scale analysis, *Proc. R. Soc. A* 465 (2009) 2089–2110, doi:10.1098/rspa.2008.0388.
- [13] C.C. Hantschk, D. Vortmeyer, Numerical simulation of self-excited thermoacoustic instabilities in a Rijke tube, *J. Sound Vibration* 277 (1999) 511–522.
- [14] J.A. Lycklama à Nijeholt, M.E.H. Tijani, S. Spoelstra, Simulation of a traveling-wave thermoacoustic engine using computational fluid dynamics, *J. Acoust. Soc. Am.* 118 (2005) 2265–2270.
- [15] G.Y. Yu, E.C. Luo, W. Dai, J.Y. Hu, Study of nonlinear processes of a large experimental thermoacoustic-Stirling heat engine by using computational fluid dynamics, *J. Appl. Phys.* 102 (2007) 074901–074907.
- [16] P. Blanc-Benon, E. Besnoin, O. Knio, Experimental and computational visualization of the flow field in a thermoacoustic stack, *C. R. Mecanique* 331 (2003) 17–24.
- [17] P. Duthil, C. Weisman, E. Bretagne, M.-X. François, Experimental and numerical investigation of heat transfer and flow within a thermoacoustic cell, *Int. J. Transp. Phenom.* 6 (2004) 265–272.
- [18] P. Le Quéré, C. Weisman, H. Paillère, J. Vierendeels, E. Dick, R. Becker, M. Braack, J. Locke, Modelling of natural convection flows with large temperature differences: A benchmark problem for low Mach number flow, Part 1. Reference solutions, *M2AN Math. Model. Numer. Anal.* 39 (2005) 609–616.
- [19] W. Briggs, *A Multigrid Tutorial*, second edition, SIAM Publications, Philadelphia, 1987.
- [20] P. Debesse, D. Baltean-Carlès, F. Lusseyran, Experimental analysis of nonlinear phenomena in a thermoacoustic system, in: *Nonlinear Acoustics – Fundamentals and Applications*, Proc. 18th ISNA, July 07–10, 2008, Stockholm, Sweden, vol. 1022, pp. 355–358.
- [21] C.H. Lees, The free periods of a composite elastic column or composite stretched wire, *Proc. Phys. Soc.* 41 (1929) 204–213.